

$^{16}\text{O} + ^{28}\text{Si}$ elastic scattering near the barrier

S. Kahana,* J. Barrette, B. Berthier, E. Chavez, A. Greiner, and M. C. Mermaz
Département de Physique Nucléaire/Basses Energies, Centre d'Etudes Nucléaires de Saclay,

91191 Gif-sur-Yvette Cedex, France

(Received 22 April 1983)

Elastic scattering angular distribution and 180° c.m. excitation function are rather well reproduced just above the Coulomb barrier by a heavy-ion nuclear potential having a repulsive core at short distances and a very strong attractive behavior at the nuclear surface. An important prediction of this potential, a precipitous drop in differential cross section at 180° , is verified experimentally.

NUCLEAR REACTIONS Prediction and observation of a simultaneous minimum in the backward angular distribution and excitation function for mass-asymmetric heavy-ion elastic scattering; signal for a molecular resonance.

The backward angle phenomenon observed in the quasi-elastic scattering of light mass-asymmetric heavy-ion systems such as $^{16}\text{O} + ^{28}\text{Si}$ is often presented as evidence for nuclear molecular behavior.^{1,2} Many models have been proposed to introduce the molecular behavior into the theoretical description of the data. However, neither the experimental nor theoretical outlines of this phenomenon have yet been completely determined. To date, many theoretical studies have been based on optical models with potentials determined parametrically from the data.²⁻⁸ As such, these models are mainly descriptive with little predictive power and do not provide a fundamental explanation of the observed phenomenon. Nevertheless, within this framework a preferred approach would be to determine the potential from the angular distribution at a single energy and then to use this potential to qualitatively describe the resonancelike structure observed in the $\theta_{\text{c.m.}} = 180^\circ$ excitation functions.^{8,9}

In this paper we report on the observation of an unusual feature supporting a molecular interpretation and predicted by a particular optical analysis which concentrated on the description of the $^{16}\text{O} + ^{28}\text{Si}$ elastic angular distribution measured just above the Coulomb barrier. At these energies the reduced density of angular oscillations seen in the backward hemisphere permits the character of these oscillations to be better defined experimentally and leads to statistically more significant optical fits. It is then easier to establish whether or not resonant behavior, localized in a few partial waves, exists and to find qualitatively important signs of these resonances. Consequently, the optical parameters are fixed by fitting the $^{16}\text{O} + ^{28}\text{Si}$ elastic angular distribution measured³ at $E_{\text{c.m.}} = 21.1$ MeV, just above the Coulomb barrier and near the first maximum in the $\theta_{\text{c.m.}} = 180^\circ$ excitation function. The optical model employed in the present analysis is somewhat unconventional.¹⁰ The values of the real potential $V(r)$ at prespecified radii (R_1, R_2, \dots, R_N) between 4 and 8 fm are themselves search parameters in the fitting routine. A linear interpolation is used for $V(r)$ between these radii, the potential is assumed to be constant for $r < R_1$, and an exponential tail $V(r)e^{-r/a}$ is tacked onto $V(r)$ for $r \geq R_N$. The imaginary part of the potential is given a more conventional volume plus surface Woods-Saxon shape. Due to the strong absorption the calculation is insensitive to the value of $V(r)$ for $r < R_1$, whereas for $r > R_N$ the low nuclear density justifies an exponential tail as predicted by folding. The resulting potential, as well as the fitted angular distribution at

$E_{\text{c.m.}} = 21.1$ MeV, are presented in Fig. 1 (see also Ref. 11). The description of the data is good with the possible exception of the neighborhood of the rainbow peak. To fit the data by the present approach it is imperative to have the small volume diffusivity indicated in Fig. 1, i.e., a surface

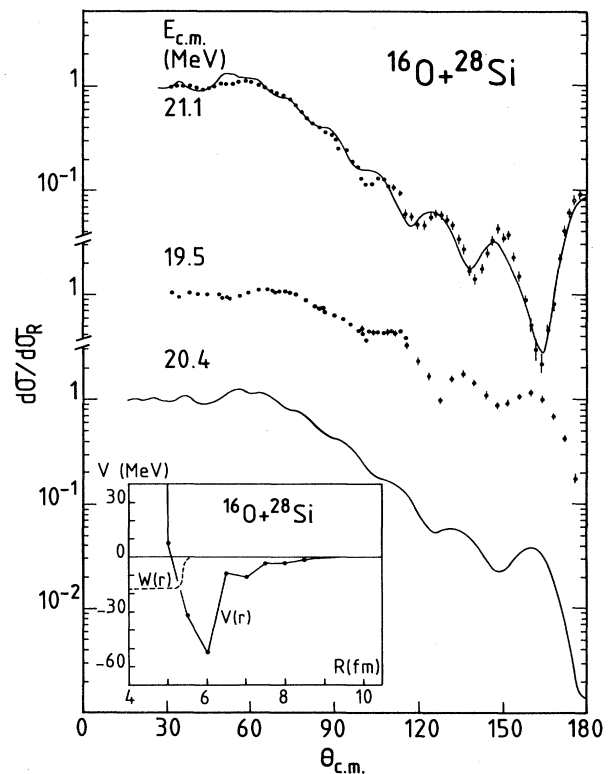


FIG. 1. ^{16}O elastic scattering angular distributions on the ^{28}Si target nucleus. Plotted in the inset is the optical model potential, real and imaginary part, used to calculate the theoretical curves. The data at 21.1 MeV determined an optical potential which was then used to predict the angular distribution of a lower energy minimum in the 180° excitation function. This minimum in the theoretical excitation function falls at 20.4 MeV, 0.9 MeV above the observed minimum at 19.5 MeV. The striking similarity between the observed angular distribution (19.4) and the theoretical (20.4), especially in the precipitous fall at 180° , indicates the presence of a resonance at this energy.

transparent interaction.

The 180° excitation function resulting from the present potential (Fig. 2) qualitatively represents the data in the low energy domain. It contains broad structures but adds an additional peak in the upper half of the region displayed. Additional structure is also predicted for energies less than 21.1 MeV. For sufficiently low energies σ/σ_R will rise to the Coulomb value of unity and the distributions are no longer oscillatory. We have not extended the calculated excitation function much above the fitting energy in accordance with our stated philosophy on low energies and because we expect, at least, the absorptive parts of the potential to change significantly with energy. The calculated resonance structure in σ/σ_R (180°) does, however, persist to quite high energy.

The original feature predicted by the present calculation is that the deep minima in the excitation function (e.g., at $E_{c.m.} = 20.4$ and 23.6 MeV) are associated with a sharp fall at $\theta_{c.m.} = 180^\circ$ in the angular distribution. For example, the calculated angular distribution at $E_{c.m.} = 20.4$ MeV is presented at the bottom of Fig. 1. To verify this important prediction a complete angular distribution was measured at $E_{c.m.} = 19.5$ MeV, at the observed minimum in the 180° -excitation function closest to the calculated minimum at 20.4 MeV. The angular distribution was obtained by standard techniques. The ^{28}Si and ^{16}O beams were provided by the Saclay FN tandem. The forward angle angular distribution in the range $70^\circ \leq \theta_{c.m.} \leq 110^\circ$ was measured with use of the ^{16}O beam and enriched ^{28}Si target of $70 \mu\text{g}/\text{cm}^2$ thick-

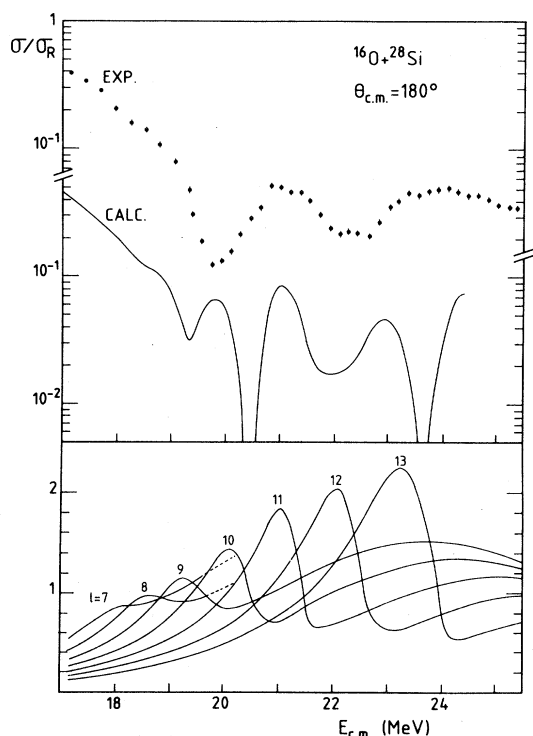


FIG. 2. $^{16}\text{O}, ^{28}\text{Si}$ elastic scattering excitation function at 180° center of mass. The theoretical curve has been computed with the optical model potential displayed in the inset of Fig. 1 with use of a modified version of the Fortran code ECIS of J. Raynal. In the lower part of the figure is plotted the nuclear phase δ_l of scattering matrix element $S_l = |S_l| \exp(2i\delta_l)$.

ness. The ^{16}O ions were detected by a position sensitive surface barrier silicon detector covering an angular range $\Delta\theta_{\text{lab}} \approx 14^\circ$. The data in the range $100 \leq \theta_{c.m.} < 180^\circ$ were obtained using the kinematically reverse reaction $^{16}\text{O}(^{28}\text{Si}, ^{28}\text{Si})^{16}\text{O}$. The ^{16}O recoil ions were detected at forward angles by the Saclay QDDD spectrometer. The absolute normalization of the data is done under the assumption that the ratio to the Rutherford cross section is one at the most forward angles. The data at backward angles are normalized in the angular range $100^\circ \leq \theta_{c.m.} < 110^\circ$ where both sets of data overlap.

The measured angular distribution is displayed in the middle of Fig. 1, and its general features, mainly the deep minimum at 180° , are in very good agreement with the calculation. The slightly different slope of the average angular distributions at large angle is entirely traceable to the somewhat different center of mass energy at which the minimum appears in the experiment and in the calculation. The fall near 180° at $E_{c.m.} = 19.5$ MeV, as well as the rises at 180° seen near maxima in the excitation function, we claim, arise from resonance-background interference and hence are strong evidence for molecularlike structure in the $^{16}\text{O} + ^{28}\text{Si}$ system.

The phenomenological theoretical basis for such an interpretation is summarized in Fig. 3 where the S -matrix amplitudes $|S(l)|$ are given for a sequence of energies, and at the bottom of Fig. 2 where the corresponding phases are shown alongside the excitation function.

The dip in $|S(l)|$ corresponds to a particularly strongly absorbed wave, while the smooth progression of this dip with energy follows an expected centrifugal dependence for the grazing wave. A viewpoint based on a single resonant

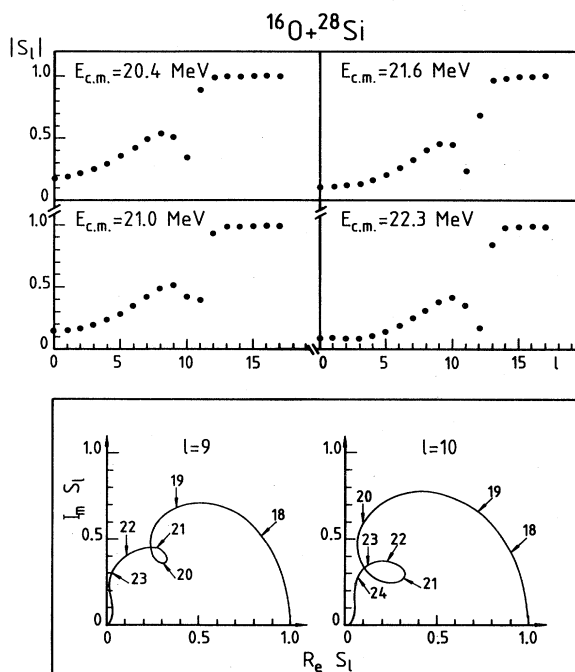


FIG. 3. General behavior of the S matrix just above the Coulomb barrier obtained with the potential plotted in Fig. 1. The energies given in the bottom of the figure are in the center of mass system. The 20.4 and 21 MeV energies correspond, respectively, to a minimum and a maximum in the excitation function.

wave is clearly oversimplified; at each energy several partial waves exhibit unusual behavior. Nevertheless, our analysis, in particular the Argand plot in Fig. 3, suggests that a resonance is actually achieved for some waves. Figures 2 and 3 indicate that the nuclear phases vary relatively little with l for the most perturbed waves. Hence the angular phase of $P_l(180^\circ)$ which varies as $(-)^l$ plays a dominant role in the resonance-background interference. This interpretation differs radically from previous treatments suggesting that resonances are present only in alternate partial waves^{2,4}; we associate resonance with both excitation maxima and minima and thus eliminate any need to insert an l dependence^{3,12} in the real optical potential. By seriously taking the notion of missing resonant waves, the study of angular distributions corresponding to minima in the excitation function was neglected and a significant feature of the low energy ion-ion interaction was passed over. Indeed, some earlier data¹³ for the heavy-ion system $^{12}\text{C} + ^{28}\text{Si}$ may have contained traces of the unusual angular distributions observed here, while Ref. 14 clearly demonstrates this behavior in light-ion scattering.

We note, in conclusion, that the shape of the real potential in Fig. 1 contains some hint of the direction to be taken for a more basic explanation of molecular states. The deep minimum at $r = 6.0$ fm is a surface contribution to the po-

tential not likely to result from a simple folding of ion densities. Appreciable deepening in the attractive ion-ion potential should arise, however, from polarization of the nuclear surfaces. A more basic treatment of the dynamics of this polarization should involve coupling to strongly excited states of the colliding ions. The absorptive potential parameters used here, in particular the very small volume diffusivity, are possibly somewhat artificial. The interior absorption at low energy is generated dominantly by fusion, while the absorptive tails could possibly be incorporated through calculation of direct and inelastic excitation processes.¹⁵

Nevertheless, this work introduces a new and unexpected element into the knowledge of ion-ion molecular states, suggestive for future studies.

We are very much indebted to Dr. J. Raynal for having modified his Fortran code ECIS to permit the use of a potential defined point by point. One of the authors (S.K.) is grateful for the hospitality afforded by the Division de Physique Théorique of the Institut de Physique Nucléaire of Orsay during part of this work. This work was partially supported by the U. S. Department of Energy under Contract No. DE-AC02-76H00016.

*Also at Département de Physique Théorique, Centre d'Etudes Nucléaires de Saclay, 91191 Gif-sur-Yvette Cedex, France. Permanent Address: Brookhaven National Laboratory, Upton, New York 11973.

¹P. Braun-Münzinger, G. M. Berkowitz, T. M. Cormier, J. W. Harris, C. M. Jachcinski, J. Barrette, and M. J. LeVine, Phys. Rev. Lett. **38**, 944 (1977).

²P. Braun-Münzinger and J. Barrette, Phys. Rep. **87C**, 209 (1982), and references therein.

³V. Shkolnik, D. Dehnhard, S. Kubono, M. A. Franey, and S. Tripp, Phys. Lett. **74B**, 195 (1978).

⁴S. Kahana, B. T. Kim, and M. C. Mermaz, Phys. Rev. C **20**, 2124 (1979).

⁵R. S. Mackintosh and A. M. Kobos, Phys. Lett. **92B**, 59 (1980).

⁶M. C. Mermaz, A. Greiner, B. T. Kim, M. J. LeVine, E. Müller, M. Ruscev, M. Petrascu, M. Petrovici, and V. Simion, Phys. Rev. C **24**, 1512 (1981).

⁷A. M. Kobos, G. R. Satchler, and R. S. Mackintosh, Nucl. Phys. **A395**, 248 (1983).

⁸J. Barrette, M. J. LeVine, P. Braun-Münzinger, G. M. Berkowitz, M. Gai, J. W. Harris, and J. M. Jachcinski, Phys. Rev. Lett. **40**, 445 (1978).

⁹M. R. Clover, R. M. DeVries, R. Ost, N. J. A. Rust, R. N. Cherry, Jr., and H. E. Gove, Phys. Rev. Lett. **40**, 1008 (1978).

¹⁰This optical model study is unpublished work by one of the authors, S. Kahana, and leans heavily on contributions from S. Pieper who developed the point by point potential search. The first fits which use this technique are published in Ref. 11.

¹¹J. Barrette and S. Kahana, Comments Nucl. Part. Phys. **9**, 67 (1980).

¹²D. Denhard, V. Shkolnik, and M. A. Franey, Phys. Rev. Lett. **40**, 1549 (1978).

¹³J. Ost, M. R. Clover, R. M. DeVries, B. R. Fulton, H. E. Gove, and N. J. Rust, Phys. Rev. C **19**, 740 (1979).

¹⁴M. Wit, J. Schiele, K. A. Eberhard, and J. P. Schiffer, Phys. Rev. C **12**, 1447 (1975).

¹⁵A. Winther *et al.* (unpublished).